Theory of induced-torque anomalies in potassium

Xiaodong Zhu and A. W. Overhauser
Department of Physics, Purdue University, West Lafayette, Indiana 47907
(Received 30 January 1984)

The nonsaturating, four-peak pattern of induced torque observed in spherical potassium samples has been a challenging puzzle for many years. It is found that this behavior can be quantitatively explained by an anisotropic Hall coefficient. This provides further confirmation of the broken translation symmetry of the ground state of potassium, i.e., a charge-density-wave structure.

I. INTRODUCTION

The nonsaturating, four-peak induced-torque patterns in potassium spheres[1,2] indicate that the Fermi surface is multiply connected and lacks cubic symmetry. Such properties are expected if potassium has a charge-density-wave (CDW) structure.[3,4] In this paper we show that the four-peaked patterns, observed between 10 and 30 kOe, can be quantitatively explained by an anisotropic Hall coefficient.

Potassium is generally considered to have a bcc crystal structure, with its Fermi surface deviating only by about one part in 10^3 from sphericity. For such a metal, the semiclassical galvanomagnetic theory[5] predicts precisely that, in high magnetic fields $\omega_c\tau \gg 1$, its magnetoresistance should saturate, and its Hall coefficient R_H should be exactly that for free electrons, i.e., $R_0=(-nec)^{-1}$. ω_c is the cyclotron frequency, τ is the electronic scattering time, and n is the electron density. Furthermore, if the induced-torque method[6] is used to measure the magnetoresistance, one expects[6,7] that the induced torque of a spherical sample will saturate for $\omega_c\tau \gg 1$. However, a large number of experiments have given totally unexpected results.

First, in all experiments the magnetoresistance $\rho(H)$ of potassium is found to increase with H, without evidence of saturation, even at fields for which $\omega_c\tau > 300$. Results obtained by four-terminal,[8] helicon-resonance,[9] and induced-torque methods[10] substantially agree. These show that $\rho(H) \cong \rho_0(1+S\omega_c\tau)$, where ρ_0 is the resistance in zero magnetic field. The Kohler slope S is typically 10^{-4}–10^{-2}, depending on sample preparation and metallurgical history. The fact that a linear behavior is found in all samples, regardless of shape, contacts, and quality, rules out explanations invoking extrinsic mechanisms such as voids,[11] inhomogeneities,[12] or surface imperfections.[13] An explanation based on anisotropic relaxation[14] also falls short by many orders of magnitude.

Second, the Hall coefficient R_H depends on the direction of $\vec{H}$ and sometimes on the magnitude too. Penz and Bowers,[9] using a low-frequency helicon, standing-wave technique, observed that $|R_H|$ decreases monotonically with increasing H. The decrease varied from sample to sample and was $\sim 7\%$ at 100 kOe. Their measurements of the absolute value of R_H showed a 6–12% enhancement over the free-electron value. However, Chimenti and Maxfield[15] found no field dependence in R_H from 20 to 100 kOe by measuring the resonances of high-frequency helicon waves in a flat plate. Nevertheless, the absolute value of R_H was larger than R_0, depending on crystal orientation. For a static magnetic field directed along a $\langle 100 \rangle$ direction, R_H was about 4% larger than R_0. For the $\langle 110 \rangle$ direction, the enhancement showed the largest deviation about 8%. Helicon resonances in a sphere[16] resulted in an enhanced R_H of 3 to 4%.

Third, the most striking effect of all, induced-torque measurements, shows dramatic angular-dependent anomalies in high magnetic fields. These anomalies will be reviewed below.

II. INDUCED-TORQUE ANOMALIES

The induced-torque method has been used to study the orientation dependence of the magnetoresistance of alkali metals. A spherical, single-crystal sample is suspended by a rod in a uniform magnetic field $\vec{H}$. As the magnetic field rotates about the suspension axis at a constant frequency Ω (typically $\Omega \sim 10^{-3}$ Hz), a circulating current is induced in the sample. This leads to an induced torque exerted on the suspension axis.

The experiments of Schaefer and Marcus[1] were the first to show anomalous high-field torque anisotropies (Fig. 1). They measured induced torques on 200 *spherical*, single crystals of potassium and observed large, twofold torque anisotropies, even when the suspension axis was parallel to a threefold, $\langle 111 \rangle$, axis. For fields below ~ 4 kOe, the twofold pattern was sinusoidal. At higher fields, four-peaked patterns emerged, as shown in Fig. 1. The occurrence of a four-peaked pattern, even when the suspension axis is parallel to a $\langle 111 \rangle$ axis, shows that the cubic symmetry has been broken. In samples for which crystal orientation had been determined by x rays, the low-field torque minima always occurred when the projection of a $\langle 110 \rangle$ axis in the horizontal plane was nearly parallel to $\vec{H}$. This indicates that the preferred axis of broken symmetry is most likely near a $\langle 110 \rangle$ crystal direction. At high fields, the torque minima increase linearly with field, but the maxima increase at a greater rate. Furthermore, the torque minima perpendicular to the preferred direction described above are always larger than the torque minima parallel to that direction.

These anomalous torque patterns were confirmed by

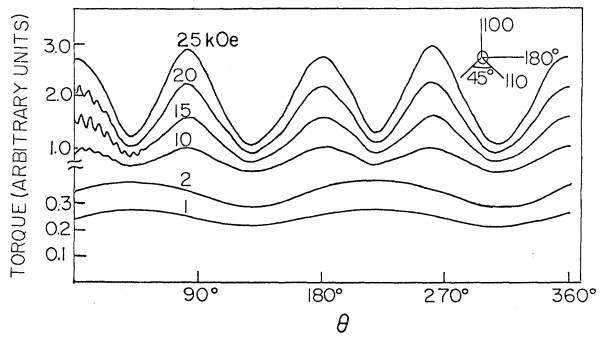

FIG. 1. Induced torque versus angle θ for a spherical sample of potassium having the $\langle 100 \rangle$ axis parallel to the suspension. The data are from Schaefer and Marcus.

Holroyd and Datars.[2] They also performed experiments on an accurately spherical sample grown in a Kel-F mold. Their data are shown in Fig. 2. In Fig. 2(a), the induced torque versus magnet angle is shown for several values of H between 500 Oe and 17 kOe. The crystal-growth axis was vertical. In Fig. 2(b), the growth axis was horizontal; and values of H range from 1 to 23 kOe in 1-kOe steps. These results are similar to those of Schaefer and Marcus in every aspect. However, the anisotropy at 23 kOe was 45:1. Schaefer and Marcus found anisotropies which ranged from 3:1 to 15:1. It should also be noted that the four peaks are not evenly spaced in angle. For example, the separation which spans the smallest torque minimum is $\sim 100°$. Unfortunately, the crystallographic orientation of this sample was never determined.

If potassium had cubic symmetry and a spherical Fermi surface, the resistivity tensor would be isotropic, and the induced torque would be independent of magnet angle θ. To explain the observed anisotropy, several mechanisms have been suggested. They can be divided into three categories.

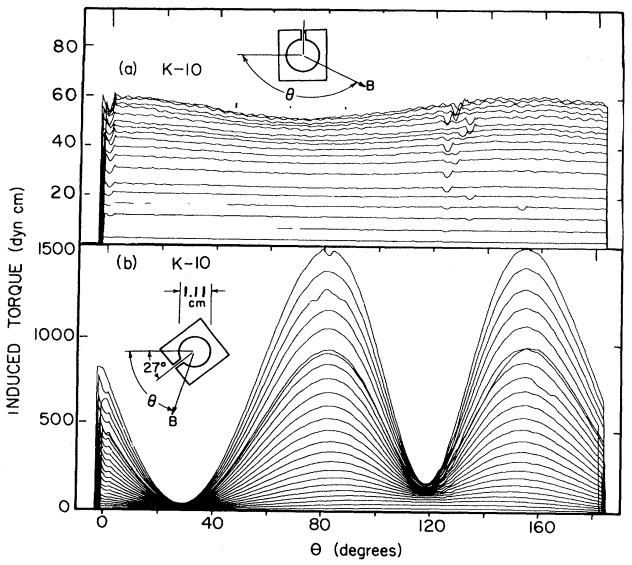

FIG. 2. Induced torque versus magnetic field direction θ for a potassium sphere 1.11 cm in diameter. In (a) the field $\vec{H}$ is rotated about the growth axis. The curves shown are for 0.5, 1, 2, 3,. . . kOe. In (b) the plane of rotation contains the growth axis, and H range from 1 to 23 kOe in 1-kOe steps. The data are from Holroyd and Datars. The crystallographic orientation is unknown.

(a) Anisotropic resistivity. Several possible causes have been considered, such as an oriented array of dislocations or voids,[11,17] or electron-phonon Umklapp processes occurring at well-defined "hot spots" on the Fermi surface.[14] However, the required concentrations of dislocations or voids exceed reasonable values by about three orders of magnitude.[2] The hot-spot model requires variations in $1/\tau$ over the Fermi surface by four orders of magnitude. Measurements[18] of phonon-scattering anisotropy reveal nothing in excess of 10%.

Even if there were a mechanism causing a large residual resistance anisotropy, say 10:1, calculation[19] shows that the induced torque becomes isotropic by 10 kOe, and a four-peak pattern does not develop.

(b) Inhomogeneous residual resistivity. We have solved the induced-torque problem for a sphere having a gradient in impurity concentration. Four-peaked patterns do not arise. This work will be published separately.

(c) Anisotropic sample shape. Lass[20] found that if a sample was sufficiently distorted from a spherical shape, the calculated torque pattern could resemble those of Schaefer and Marcus (Fig. 1). However, this explanation required deviations from sphericity of 10—15% in order to explain data such as those of Fig. 1. The measured anisotropy in shape was 2% or less.[21] The data of Fig. 2 would require a 2:1 shape anisotropy. However, this sample was spherical to a precision of $\frac{1}{2}$%. We shall show that an anisotropic Hall coefficient provides a quantitative explanation of the induced-torque patterns shown in Figs. 1 and 2.

III. MAGNETORESISTIVITY TENSOR OF POTASSIUM

We assume that the ground state of potassium has a CDW structure.[3] The conduction-electron density then has a small sinusoidal modulation,

$$\rho_e(\vec{r}) = \rho_e^0[1 - p\cos(\vec{Q}\cdot\vec{r})] , \tag{1}$$

where ρ_e^0 is the average electron density, and p and $\vec{Q}$ are the fractional modulation and wave vector of the CDW, respectively. The wave vector $\vec{Q}$ has a magnitude ~ 1.33 $(2\pi/a)$, 8% larger than a Fermi sphere's diameter.[22] The direction of $\vec{Q}$ is tilted a few degrees from a $\langle 110 \rangle$ axis and is believed to lie in a plane oriented $\sim 65°$ from the (001) plane.[23,24]

The exchange and correlation potential,

$$V(\vec{r}) = G\cos(\vec{Q}\cdot\vec{r}) , \tag{2}$$

of the CDW creates two energy gaps in $\vec{k}$ space along planes passing through $\pm\frac{1}{2}\vec{Q}$. The main gaps, about 0.6 eV,[23] distort the Fermi surface nearby, forming small necks or points of critical contact.

To maintain charge neutrality, the positive ions are displaced sinusoidally relative to their ideal bcc lattice sites $\{\vec{L}\}$. The displacements are

$$\vec{u}(\vec{L})=\vec{A}\sin(\vec{Q}\cdot\vec{L}) , \tag{3}$$

where $\vec{A}$ is the amplitude of the lattice distortion. This amplitude is 0.03 Å; the direction is parallel to the vector (18.5,54.0,53.1) if $\vec{Q}=(2\pi/a)(0.966,0.910,0.0865)$.[25] The positive-ion density $\rho_i(\vec{r})$ is

$$\rho_i(\vec{r})=\sum_{\{\vec{L}\}}\delta(\vec{r}-\vec{L}-\vec{A}\sin(\vec{Q}\cdot\vec{L})) , \tag{4}$$

where $\delta(\vec{r})$ is the Dirac δ function. We need the Fourier transform of $\rho_i(\vec{r})$,

$$\rho_{\vec{q}}=\int\rho_i(\vec{r})e^{i\vec{q}\cdot\vec{r}}d\vec{r}$$
$$=\sum_{\{\vec{L}\}}e^{i\vec{q}\cdot[\vec{L}+\vec{A}\sin(\vec{Q}\cdot\vec{L})]} . \tag{5}$$

With the use of the Jacobi-Anger generating function for Bessel functions,

$$e^{iz\sin\phi}=\sum_{n=-\infty}^{\infty}e^{in\phi}J_n(z) , \tag{6}$$

we obtain

$$\rho_{\vec{q}}=\sum_{\{\vec{L}\},n}J_n(\vec{q}\cdot\vec{A})e^{i(\vec{q}+n\vec{Q})\cdot\vec{L}} . \tag{7}$$

The sum over $\{\vec{L}\}$ yields zero unless $\vec{q}=\vec{G}-n\vec{Q}$, where $\vec{G}$ is any reciprocal-lattice vector. Since we are interested in the energy gaps which truncate the Fermi surface, we only consider those $\vec{q}$ with magnitudes smaller than the Fermi-surface diameter. The so-called "heterodyne gaps" are an important special case, corresponding to $n=1$ and $\vec{G}=\vec{G}_{110}$. For them, $|\vec{q}|\sim 0.08(2\pi/a)$.

The Fermi surface of potassium is no longer a simply connected, almost-spherical surface. It is multiply connected, with a large number of intersecting energy gaps.

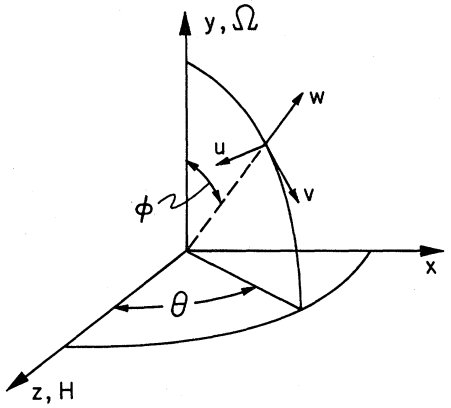

FIG. 3. Coordinate systems used in the analysis. $\hat{w}$ is parallel to the preferred texture axis for the CDW $\vec{Q}$.

In very high magnetic fields, above 40 kOe, some of the CDW energy gaps can undergo magnetic breakdown. Others will not; and as a consequence, a large assortment of open orbits come into play. The recent very-high-field, induced-torque experiments,[26] which reveal open orbits, can be explained by this model.[19] Unfortunately, the Fermi surface in lower fields, even up to 30 kOe, is quite complicated. A microscopic theory taking into account $\vec{Q}$ domains[19] and the effects of a preferred orientational texture has not been completed. Therefore, we shall postulate a phenomenological magnetoresistivity tensor, and shall attempt to justify it by qualitative arguments.

Consider a coordinate system $\hat{u}\hat{v}\hat{w}$ so that the preferred axis of orientational texture (for $\vec{Q}$) is along $\hat{w}$ (Fig. 3). In the frame shown, we assume that potassium can be described by a magnetoresistivity tensor:

$$\rho'=\rho_0\begin{pmatrix}1+S\omega_c\tau & t_1\omega_c\tau\cos\theta\sin\phi & -t_2\omega_c\tau\cos\theta\cos\phi\\ -t_1\omega_c\tau\cos\theta\sin\phi & 1+S\omega_c\tau & t_2\omega_c\tau\sin\theta\\ t_2\omega_2\tau\cos\theta\cos\phi & -t_2\omega_c\tau\sin\theta & \gamma(1+S\omega_c\tau)\end{pmatrix} . \tag{8}$$

The meaning of these quantities is as follows: γ is the ratio of zero-field resistivities parallel and perpendicular to $\hat{w}$; t_1 and t_2 describe the anisotropy of the Hall resistivity and its ratio to the free-electron value. For simplicity, we have neglected the anisotropy of the Kohler slope S, which describes the magnetoresistance. (We have verified that this is unimportant.)

It is well known that the resistivity is proportional to the weighted average of the scattering cross section $\sigma(\theta)$. The weighting factor, $1-\cos\theta$, counts 180° scattering heavily and small-angle scattering very little. For impurity scattering $\sigma(\theta)$ is sharply peaked in the forward direction, i.e., small $\vec{k}'-\vec{k}$. A CDW mixes plane-wave states $\vec{k}$ with $\vec{k}\pm\vec{Q}$. Thus, the CDW potential allows the usual wave-vector conservation rule to be supplemented by

$$\vec{k}'=\vec{k}+\vec{q}\pm\vec{Q} . \tag{9}$$

This CDW—Umklapp effect leads to a strongly enhanced large-angle scattering, but only for transitions across the Fermi surface which are nearly parallel to $\pm Q$. Accordingly, the resistivity parallel to $\vec{Q}$ is larger than it is perpendicular to $\vec{Q}$, i.e., $\gamma>1$.[27]

Energy gaps which truncate the Fermi surface cause open orbits for the conduction electrons (in a magnetic field). These lead to an H^2 magnetoresistance when $\vec{H}$ is perpendicular to an open orbit. For $H<25$ kOe the large number of open orbits (~ 120) prevents individual resolution. A magnetoresistance which is approximately linear in H results when the open-orbit effects are appropriately averaged.[19] Calculation shows that the expected Kohler

slope S is indeed about 10^{-4}–10^{-2}.

A CDW also breaks the cubic symmetry of potassium. The combination of closed orbits and open orbits (with a shorter relaxation time[19]) leads to an enhanced Hall coefficient. Indeed it will be anisotropic if the $\vec{Q}$ domains have a preferred orientation. The experiments[16] indicate (from our work) that the Hall coefficient parallel to $\vec{Q}$ is larger than the Hall coefficient perpendicular to $\vec{Q}$. Accordingly, the enhancement of t_1 over t_2 is about 10% or more. We shall assume that $t_2 \approx 1$, since we have verified that only the ratio, t_1/t_2, is relevant to anisotropic torque patterns.

IV. CALCULATION OF INDUCED TORQUE

With the resistivity tensor given by Eq. (8), and the theory of Visscher and Falicov,[7] calculation of the induced torque is straightforward. Here, it is convenient to use a magnetoresistivity tensor $\overleftrightarrow{\rho}$ transformed to the $\hat{x},\hat{y},\hat{z}$ coordinate system

$$\overleftrightarrow{\rho} = \tilde{S}\overleftrightarrow{\rho}'S \,. \tag{10}$$

The orthogonal transformation matrix is

$$S = \begin{bmatrix} -\cos\theta & 0 & \sin\theta \\ \sin\theta\cos\phi & -\sin\phi & \cos\theta\cos\phi \\ \sin\theta\sin\phi & \cos\phi & \cos\theta\sin\phi \end{bmatrix}, \tag{11}$$

where ϕ and θ are the polar and azimuthal angles of the preferred texture axis for $\vec{Q}$. The induced current, in a spherical sample of radius R, satisfying the equations

$$\vec{\nabla}\times\overleftrightarrow{\rho}\cdot\vec{j} = -\frac{1}{c}\dot{\vec{B}} \,, \tag{12}$$

$$\vec{\nabla}\cdot\vec{j} = 0 \,, \tag{13}$$

and the boundary condition

$$\vec{j}\cdot\vec{r}\,|_{|\vec{r}|=R} = 0 \,, \tag{14}$$

is of the form

$$\vec{j} = \vec{t}\times\vec{r} \,, \tag{15}$$

where

$$\vec{t} = -\left[\frac{1}{c}\right][\mathrm{Tr}(\overleftrightarrow{\rho}) - \tilde{\overleftrightarrow{\rho}}]^{-1}\dot{\vec{B}} \,. \tag{16}$$

The torque on the sample is given by the Lorentz force

$$\vec{N} = \frac{1}{c}\int \vec{r}\times(\vec{j}\times\vec{B})d^3r = \frac{1}{c}\int(\vec{t}\times\vec{r})\vec{r}\cdot\vec{B}\,d^3r$$
$$= \frac{1}{c}\vec{t}\times\left[\int\vec{r}\vec{r}\,d^3r\right]\cdot\vec{B}. \tag{17}$$

The tensor in large parentheses is the unit tensor multiplied by a factor $4\pi R^5/15$. Thus,

$$\vec{N} = (4\pi R^5/15c)\,\vec{t}\times\vec{B} \,. \tag{18}$$

Then for our system, with $\vec{B} = B\hat{z}$ and $\dot{\vec{B}} = \Omega B\hat{x}$, the torque about the $\hat{y}$ axis is

$$N_y = -(4\pi R^5/15c)Bt_x \,.$$

From Eqs. (10), (11), and (16), we may write N_y explicitly as

$$N_y = \frac{4\pi R^5\Omega}{15c^2\rho_0}\left[\frac{mc}{e\tau}\right]^2\frac{(\omega_c\tau)^2}{1+S\omega_c\tau}$$
$$\times\left[2(1+\gamma)^2+(1+\gamma)t_2^2\left[\frac{\omega_c\tau}{1+S\omega_c\tau}\right]^2(\cos^2\theta\cos^2\phi+\sin^2\theta)+2t_1^2\left[\frac{\omega_c\tau}{1+S\omega_c\tau}\right]^2\cos^2\theta\sin^2\phi\right]^{-1}$$
$$\times\left[(1+\gamma)^2\sin^2\theta\sin^2\phi+2(1+\gamma)(\sin^2\theta\cos^2\phi+\cos^2\theta)+(t_1-t_2)^2\sin^4\phi\left[\frac{\omega_c\tau}{1+S\omega_c\tau}\right]^2\sin^2\theta\cos^2\theta\right], \tag{19}$$

where we have used $\omega_c \equiv eH/mc$. The proportionality factor $(4\pi R^5\Omega/15c^2\rho_0)(mc/e\tau)^2$, which is dependent on the radius of the sample R, the rotation speed Ω, and the relaxation time τ, does not affect the torque pattern. From now on we simply omit it.

The relaxation time τ at 1.4 K is about 1.5×10^{-10} sec, which is primarily caused by impurity scattering, and is determined from the zero-field resistivity ρ_0. Accordingly, $\omega_c\tau = 50$ at $H = 20$ kOe.

Now, we are ready to discuss the torque patterns. For simplicity, we take the polar angle describing the orientation of the preferred $\vec{Q}$ direction to be $\phi = \pi/2$. (The results are similar for $\phi < \pi/2$.) In fairly low fields, $\omega_c\tau \sim 1$, the torque shows a twofold anisotropy. The maxima occur when the field is perpendicular to $\vec{Q}$ ($\theta = \pi/2$ or $3\pi/2$), and have the value

$$N_{y\,\max} \approx \frac{1}{2}\frac{(\omega_c\tau)^2}{1+S\omega_c\tau} \,. \tag{20}$$

The minima occur at $\theta = 0$ and $\theta = \pi$, and have the value

$$N_{y\,\min} \approx \frac{1}{1+\gamma}\frac{(\omega_c\tau)^2}{1+S\omega_c\tau} \,. \tag{21}$$

For larger fields, secondary minima develop where the maxima used to be, so one is left with a four-peak pattern. The torque peaks are

$$N_{y\,\mathrm{peak}} \approx \frac{(\omega_c\tau)^2}{1+S\omega_c\tau}\frac{(t_1-t_2)^2\sin^2\theta\cos^2\theta}{(1+\gamma)t_2^2\sin^2\theta+2t_1^2\cos^2\theta} \,, \tag{22}$$

which are proportional to the square of (t_1-t_2). These high-field peaks increase with H faster than linearly. The

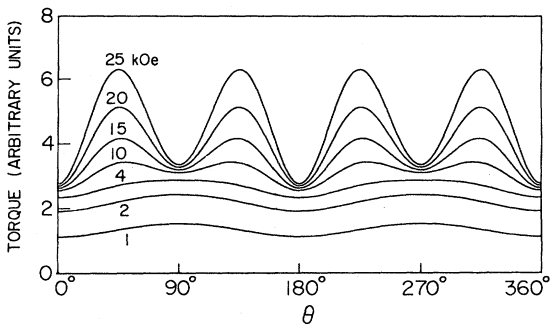

FIG. 4. Calculated induced torque versus the angle θ between $\vec{H}$ and $\vec{Q}$ for $\gamma=2.0$, $t_1=1.1$, $t_2=1.0$, and $S=0.002$.

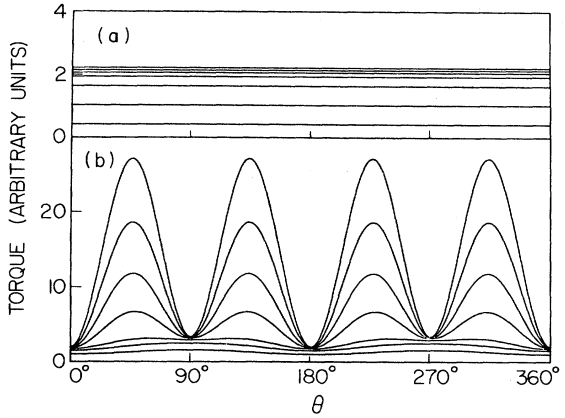

FIG. 5. Calculated induced torque versus magnetic field direction θ for $\gamma=2.0$, $t_1=1.3$, $t_2=1.0$, and $S=0.002$. (a) corresponds to magnetic fields of 0.5, 1, 2, 4, 8, 14, and 21 kOe, with $\vec{H}$ rotated about the preferred texture axis for $\vec{Q}$. In (b) the plane of rotation contains this axis, the curves shown are 1, 2, 4, 10, 15, 20, and 25 kOe.

maxima occur at angles given by

$$\theta=n\pi\pm\sin\left\{\frac{2t_1^2}{(1+\gamma)t_2^2-2t_1^2}\left[\frac{t_2}{t_1}\left[\frac{1+\gamma}{2}\right]^{1/2}-1\right]\right\}^{1/2} \quad (n=0,1,2)\,. \tag{23}$$

There are two pairs of high-field minima. The pair parallel to $\vec{Q}$ is approximately

$$N_y\approx(1+S\omega_c\tau)\frac{1+\gamma}{t_1^2}\,, \tag{24}$$

and the pair perpendicular to $\vec{Q}$ have a value of

$$N_y\approx(1+S\omega_c\tau)\frac{1+\gamma}{t_2^2}\,. \tag{25}$$

Note that these high-field minima increase linearly with H.

With $\gamma=2$, $t_1=1.1$, $t_2=1.0$, and $S=0.002$ we plot the torque curves for a series of fields. These curves are shown in Fig. 4. The fit to the curves of Schaefer and Marcus (Fig. 1) is excellent. At 25 kOe the maxima is ~1.8 times the largest minimum and ~2.3 times the smallest minimum, just as the data of Fig. 1. On remembering that the CDW vector $\vec{Q}$ is tilted a few degrees from a $\langle 110\rangle$ axis, one can understand why the high-field minima occur within 5° from parallel or perpendicular to a $\langle 110\rangle$ axis.[1]

The enormous high-field torque anisotropy reported by Holroyd and Datars should draw special attention. Since the high-field peak, Eq. (22), is proportional to the square of (t_1-t_2), it shows that for this sample the Hall resistivity parallel to the preferred $\vec{Q}$ orientation is about 30% greater than that perpendicular. On taking $\gamma=2$, $t_1=1.3$, $t_2=1.0$, and $S=0.002$, we plot in Fig. 5 the theoretical curves corresponding to Fig. 2. Apparently, the preferred texture axis for $\vec{Q}$ orientation was, in this case, the growth axis. Again, we see extraordinary agreement. For the axis of rotation parallel to the growth axis we reproduce the "flat" curves of Fig. 2. If the plane of rotation contains the axis of preferred $\vec{Q}$, an enormous high-field, four-peak pattern is produced. It is very gratifying to see that our two peaks surrounding the higher minimum (perpendicular to the preferred texture axis) are now closer than 90°; the angle between them is about 80°, which agrees with the data of Fig. 2.

V. DISCUSSION

The excellent agreement of calculated induced-torque patterns with experiment on accurately spherical samples leaves little doubt about the validity of the magnetoresistivity tensor (8). We believe that this confirms the broken symmetry of a CDW structure in potassium.

We have not yet developed a quantitative theory for a 30% anisotropy in the Hall coefficient as is required to explain the data of Holroyd and Datars. We believe that such a microscopic theory will involve *both* the shorter relaxation times for open-orbit electrons,[19] resulting from $\vec{Q}$ domain size, and the stochastic occurrence of magnetic breakdown at the many small energy gaps which truncate the Fermi surface.[28]

ACKNOWLEDGMENTS

We would like to thank Dr. M. Huberman for helpful discussions. We are also grateful to the National Science Foundation Materials Research Laboratories (NSF-MRL) program for support.

[1]J. A. Schaefer and J. A. Marcus, Phys. Rev. Lett. **27**, 935 (1971).

[2]F. W. Holroyd and W. R. Datars, Can. J. Phys. **53**, 2517 (1975).

[3]A. W. Overhauser, Phys. Rev. **167**, 691 (1968).

[4]For an experimental and theoretical review see A. W. Overhauser, Adv. Phys. **27**, 343 (1978); in *Electron Correlations in Solids, Molecules, and Atoms*, edited by J. T. Devreese and F. Brosens (Plenum, New York, 1983), p. 41.

[5]I. M. Lifshitz, M. Ia. Azbel, and M. I. Kaganov, Zh. Eksp.

Teor. Fiz. **31**, 63 (1956) [Soviet Phys.—JETP **4**, 41 (1957)]; E. Fawcett, Adv. Phys. **13**, 139 (1964).
[6]J. S. Lass and A. B. Pippard, J. Phys. E **3**, 137 (1970).
[7]P. B. Visscher and L. M. Falicov, Phys. Rev. B **2**, 1518 (1970).
[8]R. L. Schmidt, Cornell University Materials Science Center Report No. 1434 (unpublished).
[9]P. A. Penz and R. Bowers, Phys. Rev. **172**, 991 (1968).
[10]J. S. Lass, J. Phys. (Paris) Colloq. **31**, C3-1926 (1970).
[11]D. Stroud and F. P. Pan, Phys. Rev. B **13**, 1434 (1976).
[12]C. Herring, J. Appl. Phys. **31**, 1939 (1960).
[13]G. J. C. L. Bruls *et al.*, Phys. Rev. Lett. **46**, 553 (1981).
[14]R. A. Young, Phys. Rev. **175**, 813 (1968).
[15]D. E. Chimenti and B. W. Maxfield, Phys. Rev. B **7**, 3501 (1973).
[16]S. A. Werner, T. K. Hunt, and G. W. Ford, Solid State Commun. **14**, 1217 (1974).
[17]J. B. Sampselt and J. C. Garland, Bull. Am. Phys. Soc. **20**, 346 (1975).
[18]D. K. Wagner and R. Bowers, Adv. Phys. **27**, 651 (1978).
[19]M. Huberman and A. W. Overhuaser, Phys. Rev. B **25**, 2211 (1982).
[20]J. S. Lass, Phys. Rev. B **13**, 2247 (1976).
[21]A. W. Overhauser, Phys. Rev. B **9**, 2441 (1974).
[22]A. W. Overhauser, Phys. Rev. Lett. **13**, 190 (1964); A. W. Overhauser and N. R. Butler, Phys. Rev. B **14**, 3371 (1976).
[23]A. W. Overhauser, Phys. Rev. B **3**, 3173 (1971).
[24]G. F. Giuliani and A. W. Overhauser, Phys. Rev. B **20**, 1328 (1979).
[25]G. F. Giuliani and A. W. Overhauser, Phys. Rev. B **22**, 3639 (1980).
[26]P. G. Coulter and W. R. Datars, Phys. Rev. Lett. **45**, 1021 (1980).
[27]M. F. Bishop and A. W. Overhauser, Phys. Rev. Lett. **39**, 632 (1977).
[28]F. E. Fragachán and A. W. Overhauser, Phys. Rev. B **29**, 2912 (1984).